

Article

Influence of the Preparation Method of Ag-K/CeO₂-ZrO₂-Al₂O₃ Catalysts on Their Structure and Activity for the Simultaneous Removal of Soot and NO_x

Anna Cooper, Thomas E. Davies, David J. Morgan , Stan Golunski  and Stuart H. Taylor * 

Cardiff Catalysis Institute, School of Chemistry, Cardiff University, Main Building, Cardiff CF10 3AT, UK; cooperae@cardiff.ac.uk (A.C.); daviests@cardiff.ac.uk (T.E.D.); morgandj3@cardiff.ac.uk (D.J.M.); stan.golunski@care4free.net (S.G.)

* Correspondence: taylorsh@cardiff.ac.uk

Received: 8 February 2020; Accepted: 29 February 2020; Published: 4 March 2020



Abstract: Ag/CeO₂-ZrO₂-Al₂O₃, a known catalyst for the simultaneous removal of NO_x and soot, was modified by the addition of K, and was prepared using various techniques: wet impregnation, incipient wetness, and chemical vapor impregnation at different temperatures. The effect of the preparation method on catalyst activity was studied. It was found that catalysts prepared via wet impregnation, incipient wetness, and chemical vapor impregnation at 80 °C were able to utilize in situ formed N₂O at low temperatures, to simultaneously remove NO_x and soot. The difference in preparation method affected the catalyst's ability to produce and use N₂O as an oxidant for soot. The temperature at which chemical vapor impregnation was performed greatly influenced the catalyst's ability to oxidize soot. The introduction of K to the Ag/CeO₂-ZrO₂-Al₂O₃ vastly improved the soot oxidation activity, particularly for the catalyst prepared via wet impregnation. However, the incorporation of K had an adverse effect on the reduction of NO_x.

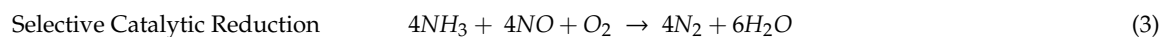
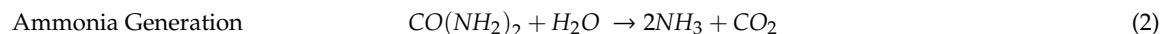
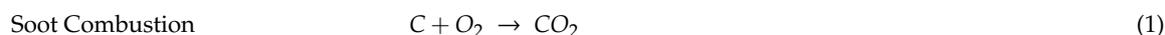
Keywords: diesel exhaust; NO_x reduction; soot oxidation; nitrous oxide; silver

1. Introduction

It is well known that emissions from vehicles are hazardous to both the environment and human health [1–3], hence the automotive industry must meet regulations in order to reduce these emissions. The four key emissions that are restricted by the EURO limits are carbon monoxide, unburnt hydrocarbons (HCs), nitrous oxides (NO_x), and particulate matter (PM) [4]. The most recent EURO limit (EURO 6) saw a 67% decrease in the permitted NO_x concentration emitted from diesel passenger vehicles, as compared to the previous limit [5]. These limits are now being rigorously enforced through on-road emission measurements as well as in laboratory rolling-road tests. Many countries are phasing out gasoline and diesel-powered vehicles in favor of electric ones, however, it will still be many years until there are no longer diesel and gasoline vehicles on the roads.

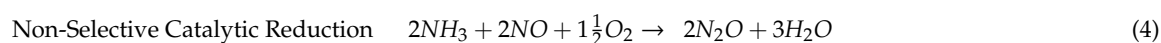
Gasoline vehicles operate under stoichiometric conditions, allowing the exhaust gas to be treated by a single catalytic converter, however, this is not the case for diesel vehicles [6]. Diesel vehicles have several exhaust aftertreatment components which remove CO, HCs, NO_x, and PM (or soot). A single aftertreatment system would increase vehicle performance due to a lower weight and back pressure, in addition to faster warm up compared to the combination of separate systems. Two of the more complex systems to combine are the regeneration of the diesel particulate filter (DPF), used to remove PM, and the selective catalytic reduction (SCR) of NO_x. The regeneration of the DPF occurs via the catalytic combustion of fuel at high temperatures, resulting in the complete oxidation of the trapped

soot (Equation (1)). However, the SCR of NO_x to N₂ using NH₃ as the reductant (which is formed in situ from aqueous urea), operates under normal exhaust temperatures, typically 100–360 °C for passenger vehicles [7] (Equations (2) and (3)).



Recently, Ag/CeO₂ catalysts have been shown to be active for soot combustion [8–14]. Ceria is a widely used support for soot oxidation catalysts, due to its ability to promote oxygen storage as well as its redox behavior [15–21]. The incorporation of Ag into the surface of ceria has been shown to greatly enhance soot oxidation, reducing the temperature required for complete soot combustion by >250 °C [12,22]. Hence, it has the potential to remove the need for fuel injection into the exhaust to regenerate the DPF in passenger vehicles. The removal of the fuel injection protocol would improve the fuel economy of vehicles and lower CO₂ emissions.

Davies et al. [23] found that an Ag/CeO₂-ZrO₂-Al₂O₃ (Ag/CZA) catalyst was active for the simultaneous removal of NO_x and soot. It was shown that the Ag catalyst could reduce NO_x to N₂ whilst oxidizing soot at low temperatures, typical of a diesel exhaust, even though the catalyst was a poor SCR catalyst in the absence of soot. This was a consequence of the production of N₂O from the non-selective SCR (Equation (4)) reaction, initiating soot oxidation at low temperatures in the presence of the Ag catalyst (Equations (5) and (6)). At higher temperatures, N₂O is no longer formed as the SCR reaction becomes more selective and hence NO_x reduction by NH₃ is dominant and soot oxidation occurs utilizing O₂ and NO₂ as oxidants.



Building on this previous work, we have been investigating the effect of the catalyst preparation method to investigate the performance for the simultaneous removal of NO_x and soot. Potassium, a well-established promoter of soot oxidation [24,25], has also been incorporated into the catalyst. There were significant differences in catalytic activity between the various preparation methods, and these are presented and discussed in this paper.

2. Results and Discussion

2.1. Catalyst Activity

Catalytic testing was carried out using a simulated exhaust gas, which deliberately excluded the major combustion products (CO₂ and H₂O) as these gases could mask small changes in the composition of the gas stream. In particular, this allowed the desorption of CO₂ from the catalyst (in the absence of soot) and its formation during the oxidation of soot to be effectively monitored.

2.1.1. Chemical Vapor Impregnation (CVI) Catalysts

The temperature at which the CVI preparation method was carried out influenced the activity towards soot oxidation and NO_x reduction (see Figure 1). The catalyst prepared at a CVI temperature of 60 °C (CVI60) proved to be a poor catalyst for NO_x reduction, with the NO concentration remaining at 500 ppm for most of the experiment until 475 °C, where the concentration increased. This increase in concentration corresponds to the decrease in concentration of NH₃, suggesting that the high temperature oxidation of NH₃ produces NO. CO₂ was first observed at 275 °C, the CO₂ trace is very similar to that observed for this catalyst in the absence of soot (see Supplementary Information,

Figure S1). This implies that the presence of the CO_2 is mainly due to decomposition of residual carbonate (which had survived the calcination treatment) or to the dissociation of surface carbonate or hydrogencarbonate species (which had formed by adsorption of CO_2 and H_2O from ambient air prior to catalyst testing).

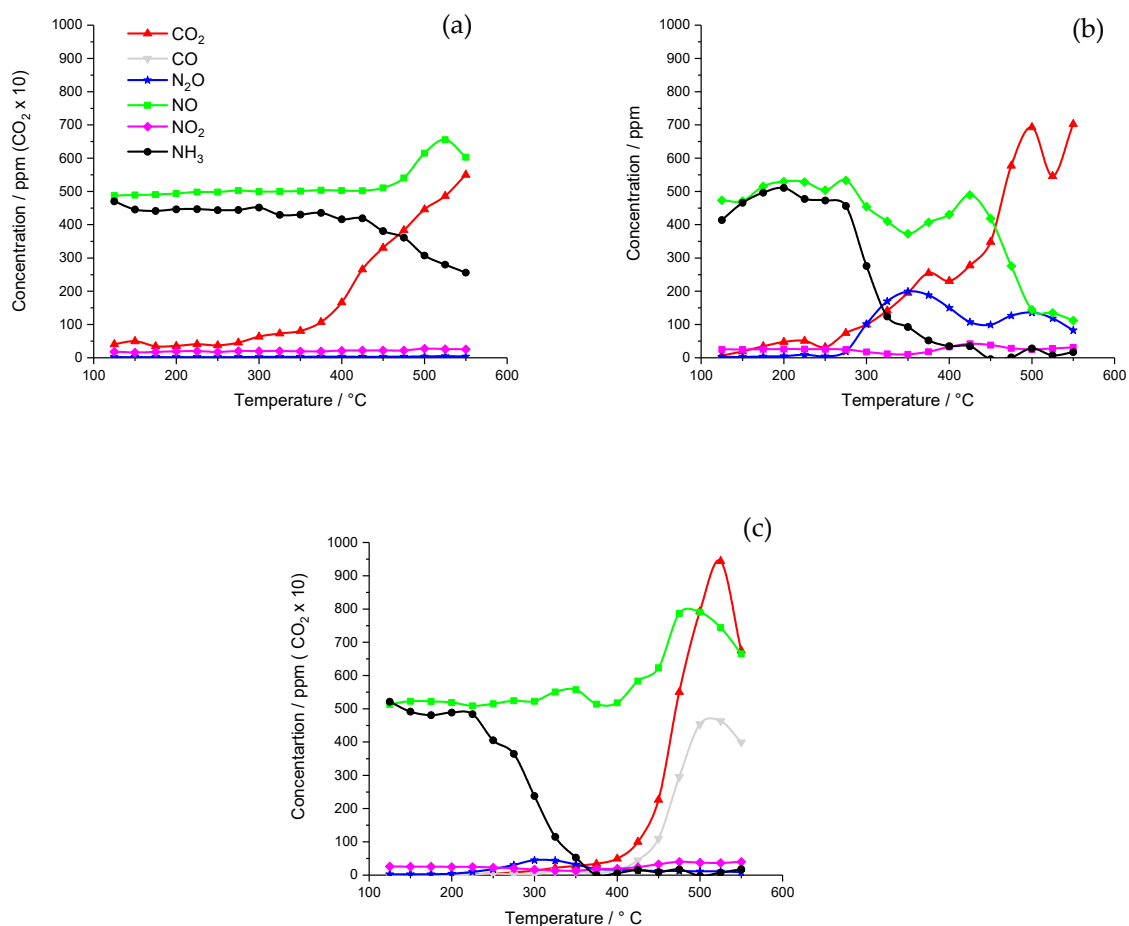


Figure 1. Variation of reactants and products as a function of temperature for NO_x reduction and soot combustion where the simulated exhaust gas consisted of 500 ppm NO , 500 ppm NH_3 , 8% O_2 , with a balance of N_2 . The temperature was increased in 25 °C intervals from 125 to 550 °C. A total of 0.25 g of catalyst was mixed in a 10:1 ratio by mass with soot. The catalysts were prepared by the following methods: (a) Chemical Vapor Impregnation (CVI) at 60 °C, (b) CVI at 70 °C, and (c) CVI at 90 °C.

CVI70 does show a reduction in the concentration of NO_x and NH_3 , but this does not occur simultaneously, this is partially due to NH_3 storage by the support, probably on Lewis acid sites (oxygen vacancies) on the CZA. The adsorbed NH_3 species can subsequently take part in the SCR reaction via a Langmuir–Hinshelwood mechanism [26]. N_2O begins to form at 275 °C but is not used to oxidize soot, as the same quantity of N_2O was formed in the absence of soot (see supplementary information, Figure S1). Similarly, CO_2 was observed from 125 °C, but again cannot be attributed to soot oxidation, as CO_2 was observed in the absence of soot, indicating the presence of residual or adsorbed carbonate or hydrogencarbonate species. At temperatures above 400 °C, greater amounts of CO_2 were observed due to uncatalyzed soot oxidation at the higher temperatures as seen in the reaction without soot (Supplementary Information Figure S1).

CVI80 showed more characteristics of the required catalytic activity. Up to 400 °C, NO_x reduction occurred, as shown by the decrease in concentration of NO and NH_3 (see Figure 2). In the absence of soot, between 250 °C and 400 °C, the N_2O trace is almost a mirror image of the inverted NO peak.

This is consistent with the non-selective SCR (Eq 4) reaction, which shows that for every mole of NO consumed there is 1 mole of N_2O formed. Between 250 and 500 °C, in the presence of soot, N_2O was observed with a maximum (approx. 150 ppm) concentration at 375 °C. This maximum is less than that observed in the absence of soot, suggesting that the N_2O is being utilized to oxidize soot. This is supported by the other reaction data, as with the decrease in the N_2O peak there is a simultaneous increase in CO_2 . In the presence of soot at 250 °C, a concentration of 70 ppm of CO_2 was measured, compared to the case in the absence of soot, which only produced 30 ppm of CO_2 at 250 °C. This implies that low temperature oxidation (<300°C) of soot by N_2O is possible using this catalyst. However, this does not account for the full decrease in the concentration of N_2O , this is due to some of the N_2O being stored by soot until higher temperatures [23]. Over this catalyst, a relatively high concentration of CO_2 was observed, particularly at high temperatures, again showing the ability of the catalyst to directly catalyze the oxidation of soot.

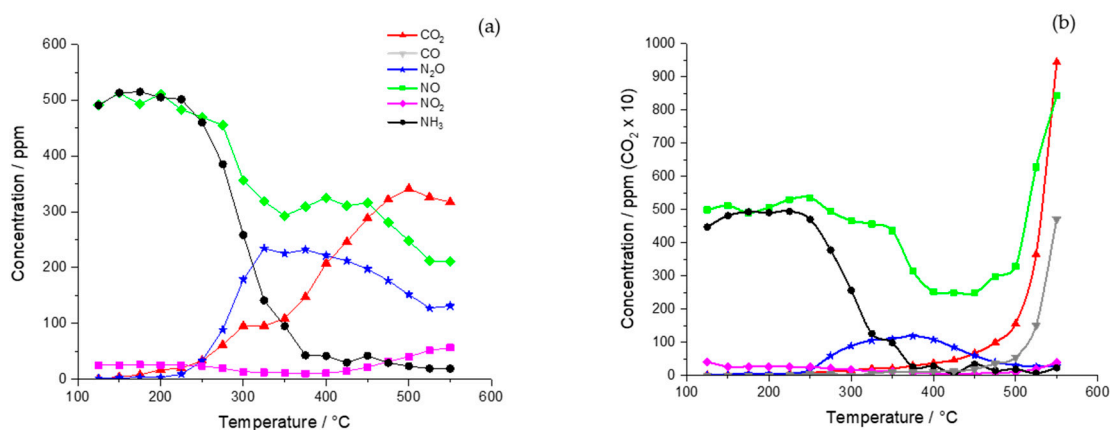


Figure 2. Reaction data for CVI80 catalyst where the simulated exhaust gas consisted of 500 ppm NO, 500 ppm NH_3 , 8% O_2 , and N_2 as the balance gas. The temperature was increased in 25 °C intervals from 125 to 550 °C. (a) catalyst only reaction data, and (b) catalyst and soot data. (Note difference in scales between (a) and (b) for CO_2 concentration.)

The CVI90 catalyst demonstrated exceptionally good activity for soot oxidation, especially at high temperatures, with CO_2 production onset at 375 °C and peaking at 500 °C with a concentration >9500 ppm. However, the NO concentration did not decrease at all during the reaction; indeed, the concentration increased at temperatures above 400 °C when NH_3 oxidation is both thermodynamically and kinetically favored. Hence, CVI90 is not a suitable catalyst for the simultaneous removal of NOx and soot but it is an effective catalyst for soot oxidation by NO_2 and O_2 .

2.1.2. Incipient Wetness Catalyst

The 2 % Ag-20 % K/CZA catalyst made via incipient wetness displayed interesting properties for soot oxidation. The catalyst used low-temperature N_2O (225–400 °C) to oxidize soot, as shown by the relative difference in CO_2 and N_2O concentrations between the reaction with and without the presence of soot (Figure 3). From Figure 3, it can be determined that, for this catalyst, N_2O is formed as a result of NH_3 oxidation, even when the NOx-reduction reaction is suppressed by the presence of soot. The catalyst also uses NO_2 at high temperatures to oxidize the soot. Despite being an active catalyst for soot oxidation at low temperatures, the concentration of CO_2 observed is significantly lower than that from other preparation methods at higher temperatures. In the absence of soot, the catalyst performs the desired NOx-reduction reaction at 125–300 °C, however, at >300 °C, the NO concentration increases as the direct oxidation of NH_3 begins to dominate. In the presence of soot, the NOx-reduction reaction does not take place; instead, the data are consistent with the NH_3 being converted through partial oxidation (to N_2O) and deep oxidation (to NO and NO_2).

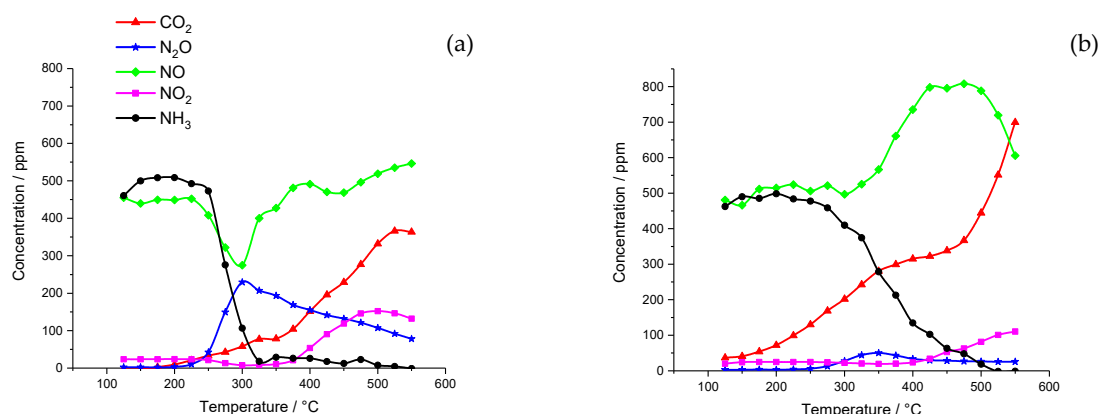


Figure 3. Reaction data for incipient wetness catalyst where the simulated exhaust gas consisted of 500 ppm NO, 500 ppm NH₃, 8% O₂, and N₂ as the balance gas. The temperature was increased in 25 °C intervals from 125 to 550 °C. (a) catalyst only reaction data, and (b) catalyst and soot data.

2.1.3. Wet Impregnation Catalyst

In the absence of soot, the wet impregnation catalyst showed good NO_x-reduction performance, with both NH₃ and NO reaching 0 ppm (Figure 4). Between 175 and 300 °C, a peak of N₂O was observed in the absence of soot. This peak was not observed when soot was introduced to the system. The absence of N₂O is consistent with the facilitating low temperature oxidation of soot. However, in the presence of soot, N₂O was observed at higher temperatures (>300 °C), probably because its formation now occurs over a temperature range where soot oxidation by NO₂ and O₂ can predominate. In the absence of soot, a large spike of CO₂ was observed at 325 °C, which corresponds closely to the decomposition temperature for Ce(CO₃)₂ [27,28], suggesting that the calcination treatments of the support and the fully-formulated catalyst had not converted all the CZA-carbonate to CZA-oxide. This CO₂ has a diluting effect on the gas stream when it desorbs, explaining the fluctuations in the NH₃, NO, and N₂O traces. When soot was introduced into the system, NO_x reduction was suppressed, but N₂O was still formed (by partial oxidation of NH₃) albeit at a higher temperature. Very high concentrations of CO₂ were detected in the presence of soot, when a step-wise oxidation of soot was observed, as described by Davies et al. for K-free Ag/CZA [23]. However, the catalyst of Davies et al. had the ability to simultaneously reduce NO_x and utilize in-situ generated N₂O to oxidize soot, whilst this catalyst is less effective for NO_x reduction in the presence of soot. This suggests that K₂CO₃ is suppressing this reaction. Overall, the performance data shows that, in the absence of soot, this catalyst is active for NO_x reduction (mainly through SCR), whilst in the presence of soot it has much lower NO_x-reduction activity but is capable of oxidizing the soot over a wide range of temperatures.

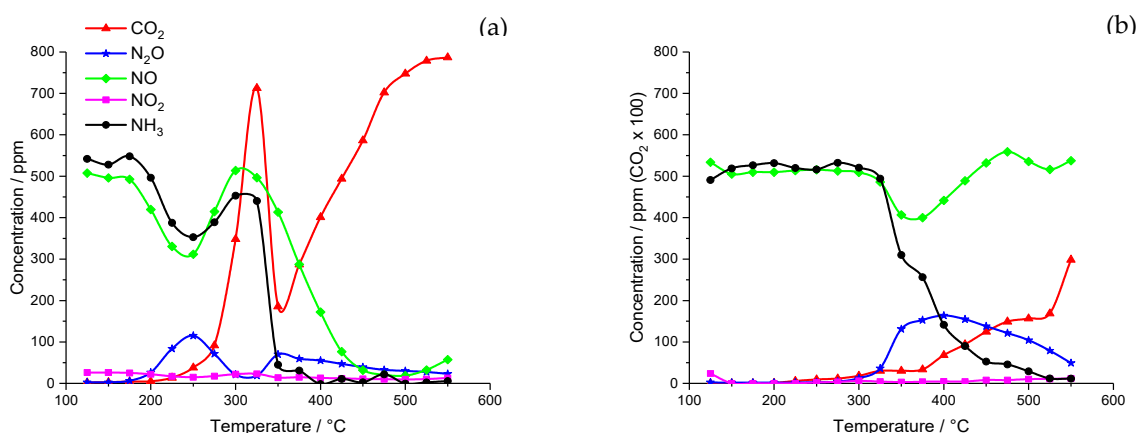


Figure 4. Reaction data for wet impregnation catalyst where the simulated exhaust gas consisted of 500 ppm NO, 500 ppm NH₃, 8% O₂, and N₂ as the balance gas. The temperature was increased in 25 °C intervals from 125–550 °C. (a) catalyst only reaction data, and (b) catalyst and soot reaction data. A total of 0.25 g of catalyst was mixed in a 10:1 ratio with soot to achieve loose contact. (Note difference in scales between (a) and (b) for CO₂ concentration.)

2.2. Catalyst Characterization

Raman Spectroscopy, X-ray Diffraction (XRD), BET surface area, X-Ray Photoelectron Spectroscopy (XPS), and Scanning Electron Microscopy (SEM) analysis were carried out on each catalyst with the key information shown in Table 1. The catalysts prepared via CVI were black in color and hence were diluted with KBr to allow a Raman spectrum to be obtained.

Table 1. Catalyst characterization data. The crystallite size calculated from XRD, the CeO₂ defect ratio obtained from Raman spectroscopy, and the catalyst surface area obtained from BET.

Sample	Ag Crystallite Size [nm]	CeO ₂ Crystallite Size [nm]	CeO ₂ Defect Ratio	Catalyst Surface Area [m ² g ⁻¹]
CVI60	59	18	-	3.8
CVI70	52	16	0.61	9.2
CVI80	40	33	0.74	11.8
CVI90	<100	>100	0.82	8.4
IW	<100	18	0.0037	12.5
IMP	32	20	-	26.4

Ceria-based soot oxidation catalysts have been postulated to have high activity due to the reversible Ce⁴⁺ to Ce³⁺ transition as well as the formation of surface and bulk oxygen vacancies [29]. It has been shown that, despite the reduction in surface area, with the incorporation of Ag into the ceria surface, an increase in catalytic activity is observed. Raman spectroscopy studies, identifying the relationship between activity and defect concentration, have shown that the increase in soot oxidation is due to an increase in oxygen vacancies on the ceria surface [30]. The preparation method effects the catalytic activity, as the greater the defect concentration in the ceria lattice, the higher the catalytic activity. Ag has also been shown to play an important role in activating molecular oxygen at low temperatures [31].

The Raman analysis (see Supplementary Information, Figure S2) showed that all catalysts had a band between 141 and 158 cm⁻¹, which is attributed to Ag lattice vibrational modes (i.e., phonons) [32,33]. The CZA support displayed a band centered at 451–469 cm⁻¹, from the F_{2g} Raman mode of ceria. The peaks present between 500 and 600 cm⁻¹ are indicative of the defect-induced mode of ceria's fluorite phase [13]. The F_{2g} peak distortion ratio was calculated for CVI70, CVI80, CVI90, and Incipient Wetness (IW) prepared catalysts using the F_{2g} peak and the distortion peak (D). It was not possible to calculate the distortion ratio for CVI60 and Wet Impregnation (IMP) due to the absence of the ceria distortion

peak. The calculated defect ratios (I_D/I_{F2g}) are shown in Table 1. The differences in the ratios show that the formation of bulk oxygen vacancies (V_{o-b}) are influenced by the different preparation techniques in this study, in agreement with previous work [11]. Additionally, the Ag species supported on ceria can lead to oxygen reverse spillover [9,10], creating V_{o-s} , which are filled by the bulk oxygen of ceria via diffusion [11]. Furthermore, a band was observed at 1052–1064 cm^{-1} for all catalysts, excluding CVI80, which is due to residual carbonate from the precipitation process using Na_2CO_3 or following the adsorption of CO_2 . From the XPS data (Table 2) it can be seen that Na is present on the surface of all of the catalysts.

Table 2. Atomic % of elements for each catalyst from XPS analysis.

Catalyst	Na	Ce	F	O	Ag	K	C	Zr	Al
CVI60	7.2	1.1	20.1	29.5	2.3	11.6	24.6	0.4	3.4
CVI70	5.9	1.1	17.0	31.8	2.4	14.2	22.4	0.3	5.0
CVI80	3.8	0.8	9.1	37.6	0.7	11.5	29.5	0.2	6.7
CVI90	3.4	0.6	5.1	32.0	0.3	7.2	47.4	0.1	4.6
IW	1.3	2.3	-	53.6	0.1	11.6	21.7	0.6	8.9
IMP	0.9	1.7	-	45.9	0.1	10.5	33.1	0.4	7.6

Figure 5 shows the powder X-ray diffraction patterns for the catalysts studied. All catalysts displayed typical diffraction peaks indexed to a cubic fluoride ceria phase, which agrees with the Raman data. The shift in CeO_2 peaks, compared to pure ceria [34], is due to the incorporation of ZrO_2 and Al_2O_3 into the ceria lattice. The peaks at $2\theta = 38^\circ$ and 44° shows the formation of metallic silver crystallites. From the XRD pattern, Ag is not present in the form of AgO , which agrees with the work of others investigating similar catalysts [8,10,11,35,36]. The three catalysts that have been shown to utilize N_2O to oxidize soot (IW, IMP and CVI80) display significantly lower intensities of the main Ag peak, hence suggesting that the Ag is less crystalline in these catalysts. From the XRD patterns, the Ag crystallite size for each catalyst was calculated using the Scherrer equation (Table 1). The catalysts, which were both active soot oxidation catalysts and had the ability to utilize in situ generated N_2O to oxidize soot at low temperatures (IMP and CVI80), had the smallest Ag crystallite sizes of 320 and 400 Å, respectively. However, IW, which is also an active catalyst for the simultaneous removal of NO_x and soot, but overall a poor soot oxidation catalyst, had a much larger Ag crystallite size (>1000 Å). There were small K_2CO_3 peaks visible for all catalysts, showing that under ambient conditions the K was present as the carbonate.

The BET analysis showed that all the catalysts had relatively low surface areas, in the range 3.8–26.4 $\text{m}^2 \text{g}^{-1}$ (Table 1). From the BET analysis, the IMP catalyst has the greatest surface area, however, there does not appear to be a direct correlation between surface area and the catalysts activity towards soot oxidation.

Figure 6 shows SEM images of the six catalysts. It is clear from the images that the preparation method has a significant impact on the morphology of the catalyst. Each catalyst, although in varying degrees, shows needle-like structures distributed over the surface of the catalyst, and, in order to determine the composition of the needle-like structures, the CZA and K/CZA supports were imaged and analyzed. Figure 7 shows SEM images for the CZA (a) and K/CZA (b) supports. The key difference between the two images is that, for K/CZA, needle-like structures are visible, which are not present for CZA. Elemental analysis from EDX showed that no K was present on the CZA support where there are no needles, but for the K/CZA support, K was clearly present as were the needle structures (see Supplementary Information, Figures S3 and S4). This suggests that the needles are rich in K. The preparation method and temperature has an effect on the morphology of the K_2CO_3 needles.

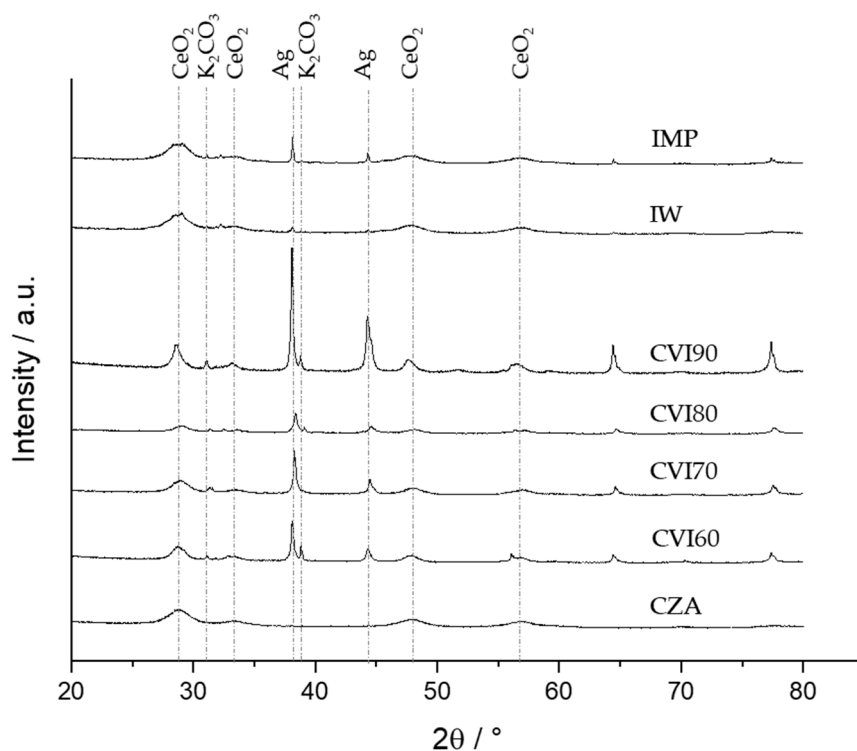


Figure 5. Powder X-ray diffraction patterns for all catalysts and for the ceria-zirconia-alumina (CZA) support.

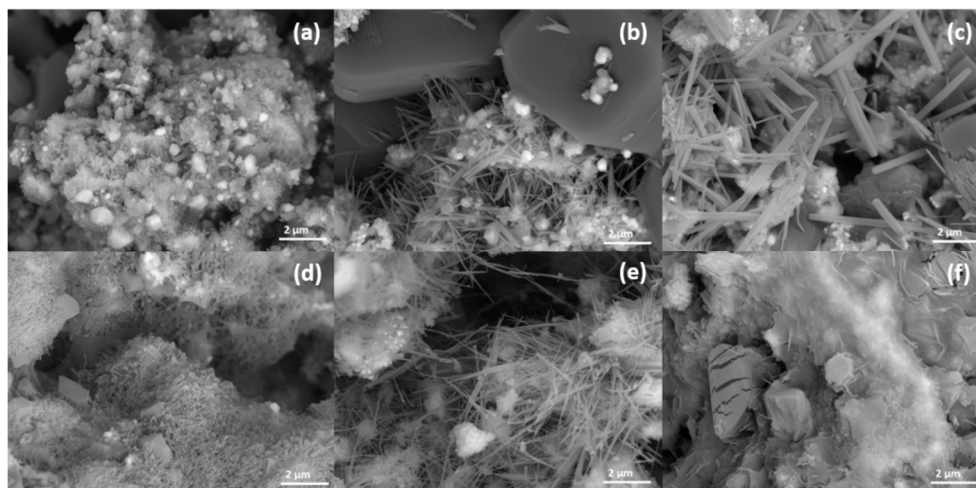


Figure 6. SEM images of the catalysts at 5Kx magnification: (a) CVI60, (b) CVI70, (c) CVI80, (d) CVI90, (e) IW, and (f) IMP.

From the images of the catalysts it can be observed that the phase separation of the CZA support has occurred as shown in Figure 6. This phase separation is observable from the pure CZA support as well as the K/CZA, hence suggesting that the preparation method is not the key factor in the phase separation. Na may also distort the measured surface concentrations of the cerium.

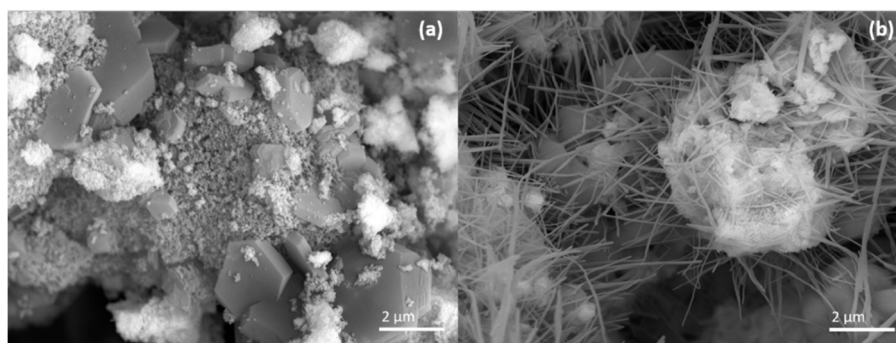


Figure 7. SEM Image at 20 Kx magnification of (a) CZA and (b) K/CZA.

The full XPS-derived surface atomic percentage concentrations for all catalyst preparations are shown in Table 2. As for EDX analysis (see Supplementary Information, Figure S5), XPS reveals the presence of significant amounts of fluorine for the CVI preparations, which was possibly unexpected and is attributed to the use of the $C_{13}H_{13}AgF_6O_2$ ((1,5-Cyclooctadiene)(hexafluoroacetylacetonato)silver(I)) precursor used to deposit Ag. The CVI preparation temperature influences the surface F concentration in the following way: as preparation temperature increases, the relative concentration of F decreases, as does Ag. XPS also confirmed the presence of high amounts of carbonate, although the concentration does vary significantly, evidenced by a C(1s) peak at ca. 289.5 eV in all spectra.

As the temperature of the CVI preparation increased, there was a decrease in the relative surface concentration of Ag, and this is most likely associated with the Ag dispersion decreasing, which is consistent with the XRD results. It is worth noting that the most active CVI80 catalyst had a low Ag surface concentration and large Ag crystallites, and the other active catalysts prepared by incipient wetness and impregnation showed the same characteristics. Hence, these catalyst features are important to utilize in situ formed N_2O at low temperatures to simultaneously remove NO_x and soot.

The oxidation state determination of Ag by XPS can be complicated due to negligible binding energy shifts between oxidation states [37]. The use of the modified Auger parameter allows for a more robust chemical assignment. Here, for the CVI60, CVI70, and CVI80 preparations, the calculated Auger parameter was 720.1 (± 0.2) eV, characteristic of metallic Ag. However, for the CVI90 catalyst, the Auger parameter was difficult to determine due to uncertainty in the absolute peak maximum, however, it is reasonable to assume that the Ag was in a similar state to the other CVI catalysts. The IW and IMP catalysts, as for the CVI90 catalysts, exhibited a low Ag concentration and a weak Auger parameter, suggesting that the Ag is present as large particles, which is confirmed by the XRD analysis.

3. Materials and Methods

The experimental study prepared 2 % Ag-20 % K/CZA by a variety of different methods (wet impregnation, incipient wetness and chemical vapour impregnation at different temperatures) and testing them for their ability to simultaneously reduce NO_x and oxidise carbon black in a simulated fuel-lean exhaust gas. Ag/CZA is a known catalyst for soot combustion as well as having the ability for simultaneously remove NO_x and soot. K is a well-known promoter of soot oxidation. The method of catalyst preparation was studied in order to establish the ideal preparation technique and to develop a deeper understanding of the properties that influence the catalyst's ability to simultaneously remove NO_x and soot.

3.1. Catalyst Preparation

3.1.1. Ceria Zirconia Alumina (CZA) Support

The CZA support was prepared by co-precipitation. Additionally, in the present study, 0.25 M solutions of ammonium cerium (IV) nitrate, zirconium (IV) oxynitrate, and aluminium nitrate nonahydrate (purity 98.5%, Sigma-Aldrich, Dorset UK; 99%, Aldrich, Dorset UK; $\geq 98\%$, Sigma-Aldrich,

Dorset UK, respectively) were used as the nitrate precursor solutions. A 1-M solution of sodium carbonate (99.5%, Alfa Aesar, Lancashire, UK) was used as the precipitating agent. This achieved an atomic composition of $Ce_{0.35}Zr_{0.15}Al_{0.5}O_{1.75}$. The resulting precipitate was filtered, washed (2 L hot de-ionised water), dried for 16 h at 110 °C, and calcined under flowing air (5 h, 10 °Cmin⁻¹, 500 °C).

3.1.2. Wet Impregnation (IMP)

A total of 2 wt% Ag–20 wt% K/CZA was prepared by dissolving AgNO₃ (99.9999%, Sigma-Aldrich, Dorset UK) and K₂CO₃ (99%, Fisher Scientific, Loughborough, UK) in de-ionized water (5 cm³). The solution was heated to 90 °C with constant stirring before the CZA support (0.78 g) was added. The solution was maintained at 90 °C and was stirred until all the excess water had been evaporated or absorbed to leave a grey paste. The solid was then dried (16 h, 110 °C) and then calcined under flowing air (5 h, 10 °C min⁻¹, 500 °C). This catalyst is referred to as IMP.

3.1.3. Incipient Wetness (IW)

A weight loading of 2 wt% Ag–20 wt% K/CZA was prepared by dissolving AgNO₃ and K₂CO₃ in minimum amounts of distilled water before the CZA support was added. The catalyst was dried (16 h, 110 °C) and calcined under flowing air (5 h, 10 °C min⁻¹, 500 °C). This catalyst is referred to as IW.

3.1.4. Chemical Vapour Impregnation (CVI)

A total of 20 wt% K/CZA was prepared via wet impregnation and dried (16 h, 110 °C) and calcined (flowing air, 5 h, 500 °C, 10 °Cmin⁻¹). Subsequently, this was shaken with C₁₃H₁₃AgF₆O₂ (99%, Sigma-Aldrich, Dorset UK) and was placed in a Schlenk flask and connected to the vacuum. The catalyst was heated to the desired temperature (60, 70, 80, or 90 °C) for 1 h. The resulting catalyst was then calcined (flowing air, 5 h, 500 °C, 10 °Cmin⁻¹). These catalysts are referred to as CVI60, CVI70, CVI80, and CVI90.

3.2. Characterization

The specific surface area was obtained by applying the BET method to a 20-point N₂ adsorption isotherm measured over the range 0.05–0.35 p/p₀ at –196 °C. The data were obtained using a Quantachrome Quadrasorb (Bracknell, UK). The catalysts were degassed under vacuum for 16 h at 120 °C before surface area analysis was carried out.

Powder X-ray diffraction was carried out using a Panalytical X'Pert diffractometer (Malvern, UK) equipped with a Cu X-ray source operating at 40 kV and 40 mA. The ICDD standard database was used for phase identification. Crystallite size was estimated by using the Scherrer equation.

Raman spectroscopy was performed using a Renishaw inVia confocal Raman microscope (Misken, Wales, UK) equipped with an argon ion visible green laser. The laser wavelength used was 514 nm and spectra were collected in reflective mode using a highly sensitive charge couple device detector. CVI catalysts were dark in colour and were therefore difficult to obtain a Raman spectrum from the pure catalysts, hence they were mixed with KBr to enable suitable spectra to be obtained.

X-ray Photoelectron Spectroscopy (XPS) was carried out on the catalysts using a Kratos Axis Ultra DLD photoelectron spectrometer (Manchester, UK) utilizing monochromatic AlK α radiation operating at an energy of 120 W (10 × 12 kV). The data were analyzed using CasaXPS (version 2.3.23, Teignmouth, UK) and were modified using Wagner sensitivity factors, as supplied by the instrument manufacturer after the subtraction of a Shirley background. All spectra were calibrated to the C(1s) line taken to be 284.8 eV.

Scanning Electron Microscopy (SEM) was performed on a Tescan MAIA3 field emission gun scanning electron microscope (Cambridge, UK) fitted with an Oxford Instruments X-ray MaxN 80 detector. The catalysts were loaded onto a carbon tape. To help prevent the charging of the samples, the catalysts were sputter coated with Au/Pd.

3.3. Catalyst Performance Testing

Previous work has established that carbon black (Cabot Black Pearls 2000, Cabot Corporation, Latvia) was a reliable diesel soot mimic [23], samples taken from a single batch were used throughout the catalytic tests in this work.

The activity of the catalysts for the selective catalytic reduction of NO by NH₃ was analyzed using a micro-reactor connected to an Fourier Transform Infra-Red (FTIR) gas analyzer (Gaset). A reactant gas mixture comprising of 500 ppm NO, 500 ppm NH₃, 8% O₂, and N₂ as the balance gas was passed over either 0.25 g of catalyst or over 0.25 g of catalyst and 0.025 g carbon black at a flow rate of 200 ml min⁻¹. Based on the catalyst volume, the GHSV for the experiments was 40,000 h⁻¹. The carbon black–catalyst mixture was prepared by mixing together with a spatula until homogenously achieving loose contact, which is comparable to the contact between a catalyst washcoat and trapped soot in a DPF [38]. For these sets of experiments, water and CO₂ were not introduced into the system to allow their formation to be detected to monitor the oxidation of carbon black. The furnace temperature was periodically increased in 25 °C increments from 125 up to 550 °C. The results from the experiments were recorded and analyzed using Origin17 (OriginLab Corporation, Northampton, Massachusetts, USA).

4. Conclusions

In this study, the effect of the preparation method for 2% Ag–20% K/CZA for the simultaneous removal of NO_x and soot from diesel exhaust by the in situ catalytic generation and utilization of N₂O was investigated. A supported Ag catalyst, known to be active from previous studies, was modified by the addition of K and prepared by wet impregnation, incipient wetness, and chemical vapor impregnation at four different temperatures. It was found that only the CVI80, impregnation, and incipient wetness catalysts utilized the in situ generated N₂O to oxidize soot at low temperatures. However, despite the incipient wetness catalyst utilizing in situ generated N₂O to oxidize soot at low temperatures, overall, it was shown to be a poor soot oxidation catalyst. The addition of K vastly improves the catalytic oxidation of soot but has a negative impact on the reduction of NO_x compared to previous work [23]. The results indicate that a 20 wt % loading of potassium is excessive, by overly hindering NO_x reduction, though still allowing N₂O to be formed directly from NH₃. Hence, a loading study is required to identify the optimum surface concentration of K for both N₂O formation by non-selective NO_x reduction and soot oxidation.

Supplementary Materials: The following are available online at <http://www.mdpi.com/2073-4344/10/3/294/s1>, Figure S1: SCR reaction data for CVI catalysts, Figure S2: EDX Map of CZA Support, Figure S3: EDX Map of K/CZA.

Author Contributions: Formal analysis by A.C., T.E.D. and D.J.M.; Investigation by A.C., T.E.D. and D.J.M.; Methodology by A.C., S.G. and S.H.T.; Supervision by S.G. and S.H.T.; Writing – original draft by A.C.; Writing – review & editing by T.E.D., D.J.M., S.G. and S.H.T. All authors have read and agreed to the published version of the manuscript.

Funding: None to acknowledge.

Conflicts of Interest: The authors declare no conflict of interest.

References

1. World Health Organization Regional Office for Europe. *Health Effects of Particulate Matter*; World Health Organization Regional Office for Europe: Copenhagen Ø, Denmark, 2013.
2. Cohen, A.J.; Anderson, R.; Ostra, B.; Dev Pandey, K.; Krzyzanowski, M.; Künzli, N.; Gutschmidt, K.; Pope, A.; Romieu, I.; Samet, V.; et al. The global burden of disease due to outdoor air pollution. *J. Toxicol. Environ. Health Part A* **2005**, *68*, 1301–1307. [[CrossRef](#)]
3. *Health Assessment Document for Diesel Engine Exhaust*; United States Environmental Protection Agency: Washington, DC, USA, 2002; Volume 67.

4. Union, T.E. Commission Regulation (EU) 2016/427-of 10 March 2016-amending Regulation (EC) No 692/2008 as regards emissions from light passenger and commercial vehicles (Euro 6). *Off. J. Eur.* 2016/427. Available online: <https://eur-lex.europa.eu/eli/reg/2016/427/oj> (accessed on 3 March 2016).
5. Dieselnet. Available online: <https://www.dieselnet.com/standards/eu/ld.php> (accessed on 28 August 2019).
6. Twigg, M.V. Catalytic control of emissions from cars. *Catal. Today* **2011**, *163*, 33–41. [[CrossRef](#)]
7. Twigg, M.V. An essay book review of ‘Urea-SCR technology for deNO_x after treatment of diesel exhausts’. *Johns. Matthey Technol. Rev.* **2015**, *59*, 221–232. [[CrossRef](#)]
8. Grabchenko, M.V.; Mamontov, G.V.; Zaikovskii, V.I.; La Parola, V.; Liotta, L.F.; Vodyankina, O.V. Design of Ag-CeO₂/SiO₂ catalyst for oxidative dehydrogenation of ethanol: Control of Ag–CeO₂ interfacial interaction. *Catal. Today* **2019**, *333*, 2–9. [[CrossRef](#)]
9. Hu, S.; Wang, W.; Wang, Y.; Xu, Q.; Zhu, J. Interaction of Zr with CeO₂ (111) Thin Film and Its Influence on Supported Ag Nanoparticles. *J. Phys. Chem. C* **2015**, *119*, 18257–18266. [[CrossRef](#)]
10. Liu, S.; Wu, X.; Liu, W.; Chen, W.; Ran, R.; Li, M.; Weng, D. Soot oxidation over CeO₂ and Ag/CeO₂: Factors determining the catalyst activity and stability during reaction. *J. Catal.* **2016**, *337*, 188–198. [[CrossRef](#)]
11. Gao, Y.; Duan, A.; Liu, S.; Wu, X.; Liu, W.; Li, M.; Chen, S.; Wang, X.; Weng, D. Study of Ag/Ce_xNd_{1-x}O₂ nanocubes as soot oxidation catalysts for gasoline particulate filters: Balancing catalyst activity and stability by Nd doping. *Appl. Catal. B Environ.* **2017**, *203*, 116–126. [[CrossRef](#)]
12. Kayama, T.; Yamazaki, K.; Shinjoh, H. Nanostructured Ceria–Silver Synthesized in a One-Pot Redox Reaction Catalyzes Carbon Oxidation. *J. Am. Chem. Soc.* **2010**, *132*, 13154–13155. [[CrossRef](#)]
13. Chang, S.; Li, M.; Hua, Q.; Zhang, L.; Ma, Y.; Ye, B.; Huang, W. Shape-dependent interplay between oxygen vacancies and Ag–CeO₂ interaction in Ag/CeO₂ catalysts and their influence on the catalytic activity. *J. Catal.* **2012**, *293*, 195–204. [[CrossRef](#)]
14. Sadlivskaya, M.V.; Mikheeva, N.N.; Zaikovskii, V.I.; Mamontov, G.V. Influence of Preparation Method of Ag–CeO₂ Catalysts on Their Structure and Activity in Soot Combustion. *Kinet. Catal.* **2019**, *60*, 432–438. [[CrossRef](#)]
15. Bueno-López, A. Diesel soot combustion ceria catalysts. *Appl. Catal. B Environ.* **2014**, *146*, 1–11. [[CrossRef](#)]
16. Peralta, M.A.; Zanuttini, M.S.; Querini, C.A. Activity and stability of BaKCo/CeO₂ catalysts for diesel soot oxidation. *Appl. Catal. B Environ.* **2011**, *110*, 90–98. [[CrossRef](#)]
17. Rao, K.N.; Venkataswamy, P.; Reddy, B.M. Structural Characterization and Catalytic Evaluation of Supported Copper-Ceria Catalysts for Soot Oxidation. *Ind. Eng. Chem. Res.* **2011**, *50*, 11960–11969. [[CrossRef](#)]
18. Muroyama, H.; Hano, S.; Matsui, T.; Eguchi, K. Catalytic soot combustion over CeO₂-based oxides. *Catal. Today* **2010**, *153*, 133–135. [[CrossRef](#)]
19. Kašpar, J.; Fornasiero, P.; Graziani, M. Use of CeO₂-based oxides in the three-way catalysis. *Catal. Today* **1999**, *50*, 285–298. [[CrossRef](#)]
20. Trovarelli, A. Catalysis Reviews Catalytic Properties of Ceria and CeO₂-Containing Materials Catalytic Properties of Ceria and CeO₂ -Containing Materials. *Catal. Rev. Sci. Eng.* **1996**, *38*, 439–520. [[CrossRef](#)]
21. Aneggi, E.; de Leitenburg, C.; Dolcetti, G.; Trovarelli, A. Promotional effect of rare earths and transition metals in the combustion of diesel soot over CeO₂ and CeO₂-ZrO₂. *Catal. Today* **2006**, *114*, 40–47. [[CrossRef](#)]
22. Ramdas, R.; Nowicka, E.; Jenkins, R.; Sellick, D.; Davies, C.; Golunski, S. Using real particulate matter to evaluate combustion catalysts for direct regeneration of diesel soot filters. *Appl. Catal. B Environ.* **2015**, *176*, 436–443. [[CrossRef](#)]
23. Davies, C.; Thompson, K.; Cooper, A.; Golunski, S.; Taylor, S.H.; Bogarra Macias, M.; Doustdar, O.; Tsolakis, A. Simultaneous removal of NO_x and soot particulate from diesel exhaust by in-situ catalytic generation and utilisation of N₂O. *Appl. Catal. B Environ.* **2018**, *239*, 10–15. [[CrossRef](#)]
24. Rinkenburger, A.; Toriyama, T.; Yasuda, K.; Niessner, R. Catalytic Effect of Potassium Compounds in Soot Oxidation. *ChemCatChem* **2017**, *9*, 3513–3525. [[CrossRef](#)]
25. Castoldi, L.; Matarrese, R.; Lietti, L.; Forzatti, P. Intrinsic reactivity of alkaline and alkaline-earth metal oxide catalysts for oxidation of soot. *Appl. Catal. B Environ.* **2009**, *90*, 278–285. [[CrossRef](#)]
26. Xiong, S.; Liao, Y.; Dang, H.; Qia, F.; Yang, S. Promotion mechanism of CeO₂ addition on the low temperature SCR reaction over MnO_x/TiO₂: A new insight from the kinetic study. *RSC Adv.* **2015**, *5*, 27785–27793. [[CrossRef](#)]

27. Titov, A.; Klimenko, M.; Goryacheva, E.; Opolchenova, N.; Stepareva, N.; Sokolova, N. Preparation of Ceria and Yttria Nanopowders via Thermal Decomposition of Oxalates, Carbonates, and Hydroxides. *Inorg. Mater.* **2008**, *44*, 1101–1104. [[CrossRef](#)]
28. Janoš, P.; Hladík, T.; Kormunda, M.; Ederer, J.; Štátn Martin, M. Thermal Treatment of Cerium Oxide and Its Properties: Adsorption Ability versus Degradation Efficiency. *Adv. Mater. Sci. Eng.* **2014**. [[CrossRef](#)]
29. Montini, T.; Melchionna, M.; Monai, M.; Fornasiero, P. Fundamentals and Catalytic Applications of CeO₂-Based Materials. *Chem. Rev.* **2016**, *116*, 5987–6041. [[CrossRef](#)]
30. Sartoretti, E.; Novara, C.; Giorgis, F.; Piumetti, M.; Bensaid, S.; Russo, N.; Fino, D. In situ Raman analyses of the soot oxidation reaction over nanostructured ceria-based catalysts. *Sci. Rep.* **2009**, *9*. [[CrossRef](#)]
31. Deng, X.; Li, M.; Zhang, J.; Hu, X.; Zheng, J.; Zhang, N.; Chen, B.H. Constructing nano-structure on silver/ceria-zirconia towards highly active and stable catalyst for soot oxidation. *Chem. Eng. J.* **2017**, *313*, 544–555. [[CrossRef](#)]
32. Martina, I.; Wiesinger, R.; Jembrih-Simburger, D.; Schreiner, M. Micro-Raman characterization of silver corrosion products: Instrumental set-up and reference database. *E Preserv. Sci.* **2012**, *9*, 1–6.
33. Bosnick, K.A. Raman Studies of Mass-Selected Metal Clusters. Doctor of Philosophy. Ph.D. Thesis, University of Toronto, Toronto, ON, Canada, 2000.
34. Bueno-Ferrer, C.; Parres-Esclapez, S.; Lozano-Castelló, D.; Bueno-López, A. Relationship between surface area and crystal size of pure and doped cerium oxides. *J. Rare Earths* **2010**, *28*, 647–653. [[CrossRef](#)]
35. Aneghi, E.; Llorca, J.; de Leitenburg, C.; Dolcetti, G.; Trovarelli, S. Soot combustion over silver-supported catalysts. *Appl. Catal. B Environ.* **2009**, *91*, 489–498. [[CrossRef](#)]
36. Castoldi, L.; Aneghi, E.; Matarrese, R.; Bonzi, R.; Llorca, J.; Trovarelli, A.; Lietti, L. Silver-based catalytic materials for the simultaneous removal of soot and NO_x. *Catal. Today* **2015**, *258*, 405–415. [[CrossRef](#)]
37. Ferraria, A.M.; Carapeto, A.P.; Botelho Do Rego, A.M. X-ray photoelectron spectroscopy: Silver salts revisited. *Vacuum* **2012**, *86*, 1988–1991. [[CrossRef](#)]
38. Neeft, J.P.A.; Van Pruijsen, O.P.; Makkee, M.; Moulijn, J.A. Catalysts for the oxidation of soot from diesel exhaust gases. II. Contact between soot and catalyst under practical conditions. *Appl. Catal. B Environ.* **1997**, *12*, 21–31. [[CrossRef](#)]



© 2020 by the authors. Licensee MDPI, Basel, Switzerland. This article is an open access article distributed under the terms and conditions of the Creative Commons Attribution (CC BY) license (<http://creativecommons.org/licenses/by/4.0/>).